POLITECNICO DI TORINO
Repository ISTITUZIONALE

Efficient sensitivity and variability analysis of nonlinear microwave stages through concurrent TCAD and EM modeling

Original
Efficient sensitivity and variability analysis of nonlinear microwave stages through concurrent TCAD and EM modeling / Donati Guerrieri, S.; Ramella, C.; Bonani, F.; Ghione, G.. - In: IEEE JOURNAL ON MULTISCALE AND MULTIPHYSICS COMPUTATIONAL TECHNIQUES. - ISSN 2379-8793. - STAMPA. - 4:(2019), pp. 356-363. [10.1109/JMMCT.2019.2962083]

Availability:
This version is available at: 11583/2778712 since: 2020-02-05T00:36:45Z

Publisher:
Institute of Electrical and Electronics Engineers Inc.

Published
DOI:10.1109/JMMCT.2019.2962083

Terms of use:

This article is made available under terms and conditions as specified in the corresponding bibliographic description in the repository

Publisher copyright

(Article begins on next page)

19 April 2024

Efficient sensitivity and variability analysis of nonlinear microwave stages through concurrent TCAD and EM modeling

Simona Donati Guerrieri, *Member, IEEE,* Chiara Ramella, *Member, IEEE,* Fabrizio Bonani, *Senior Member, IEEE,* and Giovanni Ghione, *Fellow, IEEE*

***Abstract*—An accurate, yet computationally efficient, Computer Aided Design (CAD) framework is proposed for the concurrent variability analysis of the active and a passive part of an RF/microwave nonlinear stage. Both the active and passive part are modeled, fully retaining a link to their physical and technological parameters. This allows for a global assessment of the nonlinear stage sensitivity and variability due to process variations. The active device is first modeled through Technology CAD (TCAD); then, the model is implemented within an RF/microwave Electronic Design Automation (EDA) circuit simulator through X-parameters. The passive part is modeled by means of accurate electromagnetic (EM) simulations and then taken into account in the circuit simulator through parametrized S-parameters. The method is demonstrated by analyzing a deep class AB Power Amplifier (PA) at 12 GHz in GaAs FET technology. In particular, a Monte Carlo analysis of the output power variability around the nominal value of 26.4 dBm due to technological variations of both active device and output matching network is presented. The active device variability is shown to dominate over the passive structure one, even if up to 30% of the overall variance is due to the passive elements at intermediate input power levels.**

***Index Terms*—X-parameters, Electromagnetic simulation, Nonlinear models, Nonlinear Variability, Microwave stage design**

I. Introduction

SUCCESSFUL, hopefully first-pass, design of nonlinear microwave circuits requires accurate, physically sound models for both the active devices and the passive structures involved. Deriving such models is a classical example of multi-scale and multiphysics simulation problem, due to the different spatial scales present in passive vs. active modeling and to the description of charge transport that TCAD inherently requires. Furthermore, recent technological progress towards nanometer scale gate lengths (below 100 nm) and the growing interest towards the promising GaN technology, have defined the link to fabrication tolerances and uncertainties as a new frontier for microwave device modeling [1].

Physical models, compared to the compact nonlinear active device models usually exploited in microwave circuit CAD, have the unique feature of retaining a link to the technological fabrication process. Conversely, most nonlinear models are based on equivalent circuits (e.g. the Angelov-Chalmers model for microwave FETs [2]) with elements modeled through analytic expressions whose parameters are only indirectly connected to the device physical structure. Indeed, they are entirely extracted from experimental characterizations of the device static and dynamic behaviors. Foundry compact models are thus often accurate only close to specific bias conditions (e.g. class AB PAs), and typically do not include statistical large-signal characterization. Emerging surface potential HEMT models ([3] and references therein) can potentially include a dependency to selected technological parameters, but are still far from the design level exploitation and suffer, in any case, from the need to oversimplify the device structure. A statistical nonlinear circuit model based on the Chalmers framework has been proposed in [4], with specific reference to the sensitivity and yield analysis of power stages, however limited to specific parameters of the quasi-physical, piece-wise compact model.

Besides equivalent circuit models, black-box (behavioral) approaches are also very popular in nonlinear modeling [5]. A widely adopted and promising behavioral model relies on the so called X-parameters (X-pars) [6], [7], effectively extending the usual S-parameter concept to the nonlinear case. The main advantage of X-pars is that a well defined procedure is established for their characterization, extraction and implementation in EDA tools, making this concept a new standard. The major limitation of the X-par model is that long-term memory effects cannot be handled, and the conventional X-par EDA implementation should not be used for transient simulations while in envelope simulations memory is limited to the frequency range used for the model extraction. Finally, being entirely based on measurements, black-box models are in any case characterized by a very weak connection to physical and technological parameters.

Physics-based (PB) analysis is in principle the ideal tool to retain the link between technology and circuit performance. TCAD nonlinear analysis of active devices via the Harmonic Balance algorithm has been proven to be feasible and relatively numerically efficient, thus effectively extending to the nonlinear domain the use of conventional physical models, such as drift-diffusion or energy-balance (see [8] for an introduction). Thermal analysis and trap dynamics can also be included through the Fourier heat diffusion or trap rate equations, respectively. This ultimately makes physical simulations capable to accurately reproduce effects such as power frequency conversion [9], intermodulation, noise frequency conversion [10], [11] and low-frequency dispersion effects [12], that collectively play a key role in the design of linear

This paper is an expanded version of a conference paper presented at IEEE MTT-S IMS 2019, Boston, MA.

and nonlinear microwave circuits.

As shown in [13], [14], variability and sensitivity analyses can be carried out within active device TCAD through an efficient numerical approach based on Green's Functions, evaluated with the so-called small-signal large-signal conversion matrix [15]. However, the main issue behind PB analysis, beyond its numerical burden, is that PB models are not usually provided as a part of foundries' design kits and cannot be easily linked to current EDA tools. This makes the information from PB analysis not directly available to the circuit designer.

To overcome this issue, we notice that frequency-domain physical simulations can be used to create the same set of data as the one extracted from measurements carried out on an active device, including e.g. scattering parameters, $P_{\text{in}}-P_{\text{out}}$ and load-pull data. Hence, any black-box model based on measurements can also be extracted from PB analysis. Along this line, we proposed in [16] X-pars as a viable way to translate PB simulations into EDA tools. Furthermore, we presented in [16] several approaches to make X-pars dependent on technological parameters, ultimately allowing for a truly physically sound EDA-oriented active device nonlinear model. Of course, X-parameters per-se are not suited as a general-purpose, scalable device compact model. On the contrary, they must be regarded as a local model, inherently limited to a given device structure and operating condition. On the other hand, for a given application (e.g. the design of a power stage with a given device periphery as in this paper) they offer a ready-to-go model to be directly included at the design level, with enough flexibility to account for device and matching network spread originating from technological variations, as demonstrated in the following Sections. Furthermore X-parameters can also be used in a hybrid way, coupling the experimental characterization of a nominal device with the statistical model from calibrated TCAD simulations [16].

Besides for active devices, sensitivity analysis is also a fundamental step in passive matching network design. However, while electromagnetic simulations are used to assess the actual behavior of passive structures and to optimize the final layout (to minimize crosstalk and fine-tune impedance matching), their numerical burden still limits the use in statistical simulations. Such simulations typically rely on equivalent circuit models, which do not accurately account for EM parasitic/coupling effects. As a consequence, also passive part models in classical PA design suffer from the lack of direct links to physical or technological parameters. To overcome this limitation, we propose here to adopt a similar approach as that exploited for active devices, relying on EM simulations and parametrized S-parameters to provide a technology-dependent black-box Microwave Data Interface Files (MDIF) model of a passive structure.

In this paper, we extend the approach in [16] by coupling the active device X-par model with accurate EM simulations of the passive layout, allowing for the multiphysics and multiscale simulation of the technological variability of a nonlinear stage in standard RF/microwave EDA tools (see Fig. 1).

We introduce in Section II the device used as an example along with the power amplifier output stage designed around it. In Section III the method proposed in [16] to identify X-pars from PB analysis is reviewed, along with the implementation of technological parameters dependent X-pars. In Section IV the optimum harmonic loads are synthesized by means of a matching network, and EM simulations are presented as a function of a geometrical parameter variations. Finally, in Section V the analysis of the PA stage with concurrent parametric variations in the active and passive part is presented.

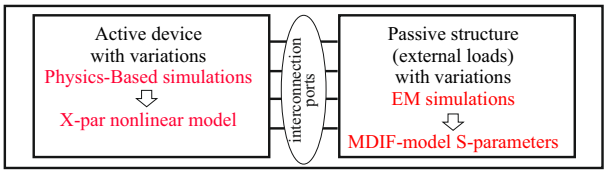

Fig. 1. Multiphysics and multiscale variability analysis of nonlinear stages.

II. The stage under study

For the sake of concreteness, we hereafter consider an epitaxial microwave power MESFET built on a 100 μm GaAs substrate. The channel layer is 0.17 μm thick with nominal doping $N_{\text{D}} = 2 \times 10^{17}$ cm^{-3}. The gate length is 0.5 μm, and a 3 Ω/mm source/drain contact resistance is considered. Physical simulations of the active device have been carried out in 2D and scaled to a 1 mm gate periphery. This value is appropriate for the final stage of a III-V medium power amplifier. Hence, the reference plane for the X-par model extracted from TCAD simulations is the nearly-intrinsic device, padded with parasitic resistances. Concerning reactive parasitics, we assume that they can be represented by a lumped LC circuit, as customary for III-V devices, directly extracted from cold-FET measurements. These lumped parasitics are usually embedded in the design of the matching network. In this preliminary analysis the details of the multifinger layout (10 fingers) have been omitted in the simulations, and may be addressed at a higher level of accuracy by coupling EM simulations with TCAD analysis, as demonstrated e.g. in [17], [18].

In this paper we address the design flow of a deep class AB tuned load power amplifier (PA) stage at 12 GHz fundamental frequency, with DC quiescent current equal to 10% of I_{DSS}. The PA circuit includes the drain matching network for optimum output power while, for this preliminary model investigation, the gate input port is left unmatched (50 Ω at all harmonics). The optimum load $(43 + \text{j}10)\ \Omega$ has been obtained by preliminary TCAD load-pull simulations at the fundamental frequency. Of course TCAD analysis already includes the effect of the intrinsic capacitances, while in this device and at this frequency, the parasitic embedding network is playing a limited role. The optimum load has been approximated to a short circuit at higher harmonics, in order to avoid the very time-consuming harmonic load-pull simulations at TCAD level.

The purpose is to perform a complete assessment of the PA sensitivity versus the concurrent variations of the active device physical parameters and of the matching network passive structure. In this analysis, the active device will be considered subject to doping variations of the channel layer while the

passive structure will be subject to variations of the thickness of the dielectric layer used for the MIM capacitors, causing a corresponding spread in the device output loading conditions. Details can be found in the following Sections.

III. Variability-aware Active Device Model: Parametrized PB X-parameters

The X-par model expresses the reflected waves at the device ports at all generated frequencies as a function of the incident waves, thus extending the concept of S-parameters to the nonlinear large-signal (LS) regime. An incident wave at fundamental (angular) frequency ω of large amplitude a_{11} at port 1 drives the system into a nonlinear LS operating condition, while all other incident waves a_{ql} (port q and harmonic l) are considered as perturbations. The reflected waves b_{pk} at port p and harmonic k

$$b_{pk}(|a_{11}|,\omega) = \sum_{q} \sum_{l=1,\dots N} S_{pq,kl}(|a_{11}|,\omega) P^{k-l} a_{ql}$$

$$+ \sum_{q} \sum_{l=1,\dots N} T_{pq,kl}(|a_{11}|,\omega) P^{k+l} a_{ql}^{*} + FB_{pk}(|a_{11}|,\omega)$$

are a superposition of LS contributions $FB_{pk}(|a_{11}|,\omega)$ and of perturbations: the key feature of the X-par model is that, to differentiate the contributions from the upper and lower sidebands of each harmonic, the effects of the incident wave a_{ql} and of its complex conjugate a_{ql}^{*} are treated independently, giving rise to two separate contributions to the back-scattered wave b. These two terms are identified by the so-called S-type and T-type X-pars, and are characterized by a different phase term ($P = \exp(\mathrm{j}\angle a_{11})$) [6]. The DC part of the variables is either the DC current, if the port is driven by a DC voltage, or a DC voltage, if the port is current driven. In this work we focus on FET devices, hence the device is driven by a gate and a drain voltage port. The DC current of each port is further divided into the LS part and the part resulting from conversion from higher harmonics, i.e. the small-signal (SS) contribution proportional to the SS incident power waves. Although the corresponding representation is mixed (scattering-admittance), the relevant terms are sometimes improperly defined as Y-type conversion terms. Analogously, Z-type terms are used for current driven ports. Collecting the DC components and the waves components FB, S, T as a function of the input large-signal incident wave $|a_{11}|$ (input available power), a lookup table model is generated and stored in a standard form, the X-par representation, for inclusion into EDA software. Here we explicitly refer to the X-par patent from Keysight [19] (*.xnp* file format), as we use Keysight ADS as the simulation environment for all the following circuit analyses[1]. The characterization is carried out by applying to each port and each harmonic the reference resistance of 50 Ω.

The X-par definition is based on a linear perturbation of the reflected waves due to the presence of (small) incident waves. As a consequence, a one-to-one relationship exists [21] with the concept of conversion matrix (CM) [22]. This is the key point allowing to extract the X-par model from PB simulations. In fact, the computation of the CM was introduced within the framework of TCAD simulations in [8] and was later extended to device variability and sensitivity analyses in [9], [13], [14], [23]. For implementation reasons, the CM evaluated into TCAD tools is defined with reference to a bilateral spectrum, so that the harmonic index runs from $-N$ to N. Furthermore, the frequency offset taken into account is positive, so that upper sidebands *only* are actually involved. However, spectral symmetry implies that the *upper* sideband of a negative frequency harmonic $p < 0$ corresponds to the *lower* sideband of harmonic $-p$ for the unilateral spectrum. In other words ($k, l > 0$)

- $S_{pq,kl}$ is obtained transforming into scattering parameter the (k,l) element of the TCAD admittance CM
- $T_{pq,kl}$ is obtained transforming into scattering parameter the $(k,-l)$ element of the TCAD admittance CM.

In the perspective of retaining the link with technological features, it is necessary to make the X-par model dependent on relevant physical parameters, such as doping concentration, gate length or trap density. In [16] two methods have been proposed to keep trace of physical parameters. In this work we exploit only the one sketched in Fig. 2, where the particular case of a two port device (4 ports in the X-par model – two RF ports + 2 DC ports), is converted into a 5 port. An extra fictitious DC port is added, isolated from all others, whose DC voltage is associated to the physical parameter to be varied (in the figure the doping DOP of the active FET channel). The model is identified by repeating the PB simulations over a prescribed set of doping values, and by extracting the X-par model parameters for each value. Then the X-pars are conveniently stored in a unique *.xnp* file as a function of the extra DC voltage port (representing the parameter), thus allowing for interpolation.

Once the X-par active device model is derived, the full capabilities of ADS can be used for a complete statistical analysis of any circuit including the same active device. In fact, the physical parameters are represented by a DC voltage and can therefore be made statistically varying, as all the other circuit parameters. Since the X-par dependence on doping is obtained through interpolation over a finite and limited – due to the PB analysis burden – set of values (here 5, spanning between -10% and $+10\%$ doping variations, it is mandatory to test whether also with random doping values the model still reproduces the original TCAD physical simulations. To this aim, we have performed an X-par ADS Monte Carlo analysis with 50 doping level samples taken from a Gaussian distribution; the spread (variance) is 5%, a quite large value chosen to verify the accuracy of the modeling strategy. The random samples generated within ADS are then exported, and TCAD analysis with the same doping concentrations is performed for validation. The simulation has been carried out both within ADS and TCAD simulators with the drain port loaded by ideal tuners, representing the optimum fundamental load and shorted harmonics. Interpolation of X-parameters over doping was implemented in ADS selecting, among the

[1]The X-parameter is a Keysight trademark, implemented into the proprietary ADS environment. However, a compatible implementation is available also within NI AWR [20], with a specific component named "XPARAM" (Nonlinear Behavioral Model Compatible with Agilent's X-parameters®).

possible options, cubic splines and constant extrapolation. Notice that with the given gaussian distribution, most the doping samples fall within the interpolation domain $[-10\%, +10\%]$ and limited extrapolation is needed. Fig. 3 shows the distribution of the output power (in dBm) resulting from the above doping variations. The ADS simulations require approximately 2 minutes, whereas the physical analysis requires more than two days of simulation time: the accuracy shown in Fig. 3 is remarkable, at all levels of input power. The main feature is that the tuned load class AB stage behaves quite differently as a function of back-off: for low input power (-3 dBm to 7 dBm input power in the figure) the output power distribution is strongly skewed towards negative values, while the input doping distribution is strictly symmetric (Gaussian). The output power distribution becomes more symmetrical as the device turns on (15 dBm) and behaves like a class A stage, however with a larger spread. Close to compression, instead, the variation is minimal. This behavior needs to be considered when the device is used in strong back-off, since the effects of variations are most important in this operating condition. Fig. 4 shows the quantile-quantile (Q-Q) plot of the output power resulting from ADS and PB analyses: again, the X-par model shows extremely good accuracy compared to PB simulations, and both deviate from the normal distribution (the reference straight line) due to the pronounced skew (especially at low input power).

As a final remark, notice that the load condition used in the above analysis is not the same as the the one used for X-parameter extraction, i.e. 50 Ω (real) at all frequencies. In fact, the optimum load has a real part of about $40\,\Omega$ (20% variation), and an imaginary part of 10 Ω. X-parameters are thus capable to reproduce the device behavior on a load (and working point) different from the reference one, at least within the range required for the present design. This result is expected to hold true even for stages similar to this one, e.g. for similar operating classes (class A to AB) and device peripheries. Of course, for extremely reduced device peripheries (e.g. below 200 μm) or higher PA classes (e.g. class F), the reference impedance for the correct X-parameters extraction may significantly deviate from 50 Ω, but this is beyond the scope of this paper, and does not affect the validity of the proposed approach.

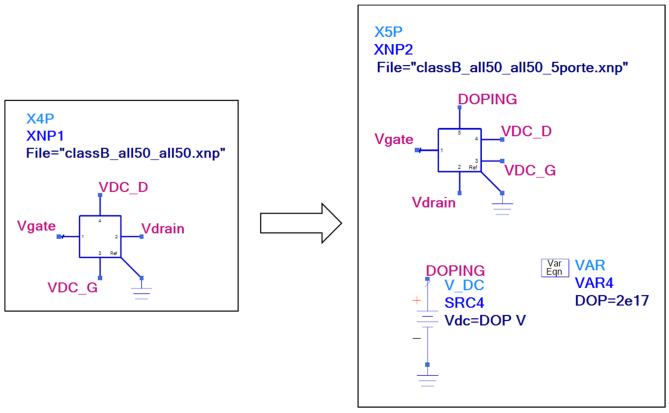

Fig. 2. X-par with extra port DOPING used for interpolation over physical parameters in the X-par file. In this example the original 4-port component (two DC and 2 RF ports) becomes a 5-port: the extra port allows doping dependent analysis.

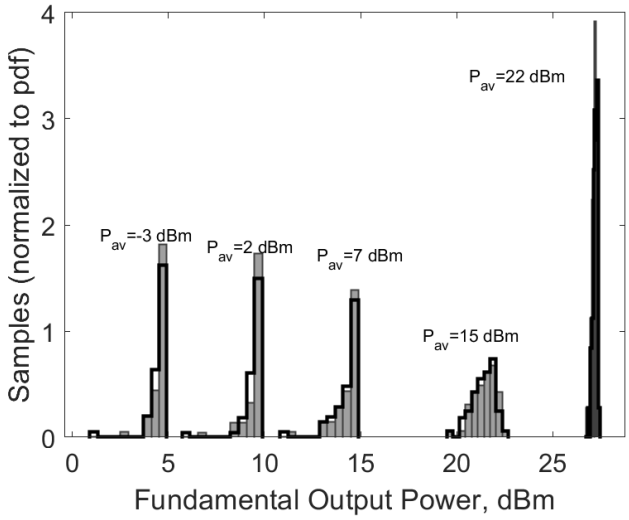

Fig. 3. Histograms of the output power (dBm) of the class AB stage as a function of random doping variations at varying input power. Shadowed: ADS Monte Carlo analysis with 50 samples. Solid lines: TCAD Monte Carlo analysis carried out on the same doping samples.

IV. Variability-aware Passive Structure Model from EM Analysis

In the previous Section, all analyses have been carried out with ideal tuners at the device drain port, providing the correct optimum load at the fundamental frequency and short-circuit conditions at higher harmonics. Following the typical design flow of a tuned load power amplifier, the matching network is now synthesized in order to control the largest possible harmonic order. Considering the typical integrated microstrip implementation on a GaAs substrate, we start with a preliminary matching network made of ideal distributed transmission lines (see Fig. 5), controlling up to the fifth harmonic. To test the model, the impedance seen at the drain port by loading this matching network is calculated up to the tenth harmonic and implemented by means of ideal tuners in the TCAD physical simulator. The agreement found is again very good, as shown for example in Fig. 6, despite the load differs at all harmonics from the 50 Ω condition used for X-par extraction. We can thus conclude that the X-par model is well verified in operating conditions close to the ones used in the final design, and proceed to the design of the microstrip network.

In order to avoid too long transmission lines, the preliminary matching network of Fig. 5 is first converted into a semi-lumped circuit, exploiting MIM capacitors to shorten both the stubs and the series lines, and then fine tuned to achieve proper loads up to the fifth harmonic. Finally, the design is converted into the corresponding layout for the final EM simulation (Fig. 7). For the passive part design and EM simulations we

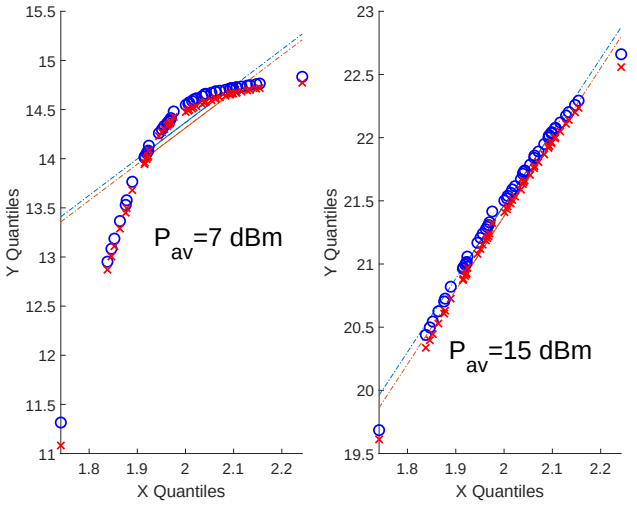

Fig. 4. Q-Q plot of the output power (Y-quantiles) vs. doping (X-quantiles). ADS (blue circles) and TCAD physical analysis (red cross) show a very good agreement. The distribution strongly deviates from the normal one (reference straight line) at low input power.

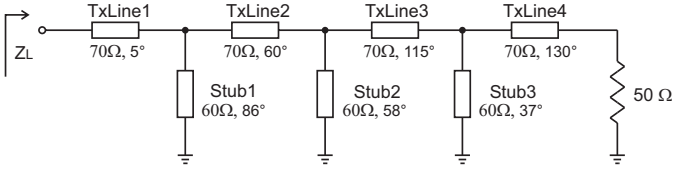

Fig. 5. Tuned load matching network with ideal transmission lines: the matching network controls up to the fifth harmonic.

adopted a technology stack-up derived from a typical GaAs design kit suitable for X-band applications, featuring two gold layers (1 μm and 2 μm thick) combined together in micro-strip transmission lines, and a 100 nm-thick SiN insulating layer for MIM capacitors (resulting in about 600 pF/mm^2 capacitance per unit area).

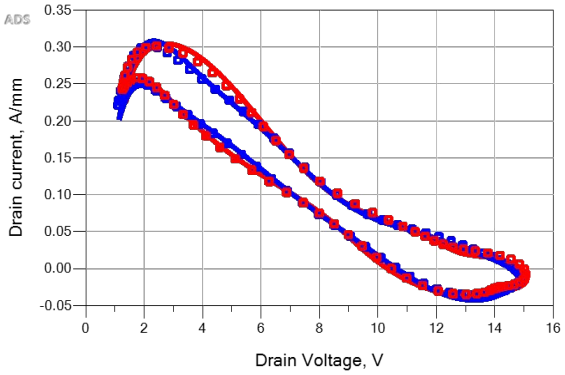

Fig. 6. Comparison of the DLL lines on the ideal optimum load (blue) and on the loads synthesized by the matching network of Fig. 5 (red). Solid lines: ADS X-par model. Symbols: Physics-based TCAD simulations. The input power is 22 dBm, driving the device well into compression.

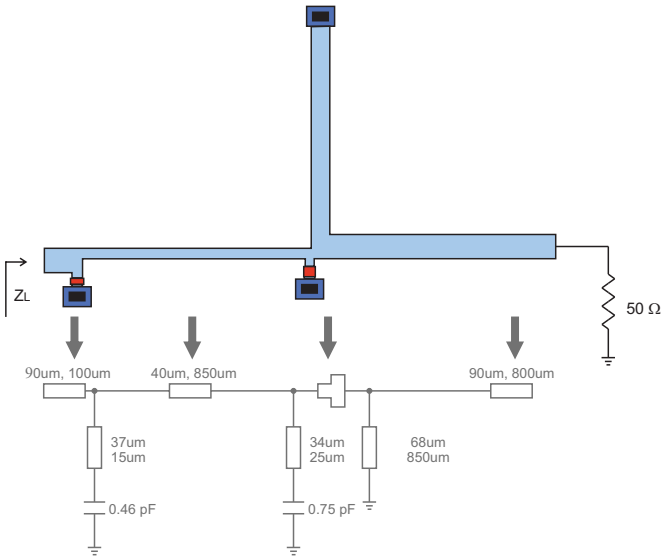

Fig. 7. Layout of the final optimized matching network.

For the sake of simplicity, and also to retain the model accuracy provided by the design kit used to derive the stack-up, EM simulations were carried out within ADS, through the full-wave planar-3D Momentum simulation engine. Nonetheless, the proposed method can be used also in conjunction with full-3D external EM simulators, as the final passive network model will be lookup table-based.

In assessing the dependence of the final PA stage on the uncertainty of the passive structure parameters, we focus on the variability of the thickness of the dielectric layer in MIM capacitors. According to the foundry specifications, the thickness of such layer is subject to variations estimated about $\pm 2\%$. In Monte Carlo analysis, the suggested spread is assumed Gaussian with 2 nm standard deviation around the nominal thickness of 100 nm. To estimate the sensitivity of the load seen by the active device due to this uncertainty, we run EM simulations for the nominal dielectric thickness and for other 6 values, corresponding to a variation of $\pm\sigma$, $\pm 2\sigma$, $\pm 3\sigma$ (where $\sigma = 2$ nm is the suggested 2% foundry standard deviation). Fig. 8 shows how the loads at the first 5 harmonics vary as a function of the simulated thickness. The variation of the fundamental load of the active device is especially significant, however the non-ideal behavior of the higher harmonics also plays a non negligible role. Notice that, despite the optimization procedure carried out to limit the impedance seen at higher harmonics, the fourth harmonic termination in particular is quite far from the ideal short circuit condition.

The EM simulation took approximately 15 minutes for each dielectric layer thickness, which is a computational time too large to make direct EM statistical analysis practically effective in a circuit CAD environment. Thus, also for the passive parts, the goal of this work is to extract a model that can be run in a circuit simulator, with no need to repeat the time-consuming physical/EM analysis. To this aim, we again choose a lookup table model, parametrized as a function of the

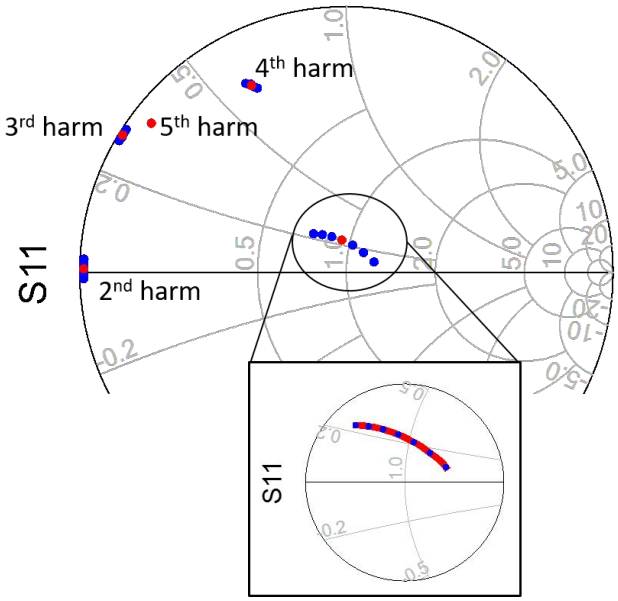

Fig. 8. Variation of the load impedance resulting from a spread of the MIM dielectric thickness. Blue marks: load impedance resulting from EM simulator with a MIM thickness variation of $\pm\sigma$, $\pm 2\sigma$, $\pm 3\sigma$ ($\sigma = 2$ nm). Red mark: nominal thickness. In the inset: fundamental frequency impedance. Blue marks: EM simulations as before, used for the MDIF dataset. Red line: ADS MDIF interpolated model with the MIM thickness varying between 94 and 106 nm.

physical parameter – here the MIM dielectric thickness – for further inclusion into ADS exploiting the internal lookup table interpolation capabilities. Since the passive structure is linear, a much simpler model can be used, replacing the active device X-par description. We exploited an *S2PMDIF* component, essentially a 2 port S-par model that allows parametrization over an external quantity via the MDIF standard.

We have therefore created a *citifile* implementing the MDIF model, based on the 7 sets of scattering parameters computed by EM simulations (namely, the nominal plus $\pm\sigma$, $\pm 2\sigma$, $\pm 3\sigma$). The inset in Fig. 8 shows that the MDIF model can continuously interpolate over the dielectric thickness, in the entire considered range. The same accuracy demonstrated in Fig. 8 for the fundamental frequency is also verified for the higher harmonics (not shown for brevity).

We can finally proceed to the Monte Carlo analysis of the matching network subject to random variations of the MIM capacitor layer: Fig. 9 shows the expected real and imaginary part of the fundamental load. As in the previous statistical analysis, we have used ADS interpolation by cubic splines and constant extrapolation. Also in this case the statical distribution of the samples over 3σ requires negligible extrapolation. Notice that the Monte Carlo analysis carried out in ADS via the MDIF model over 250 samples is nearly instantaneous. A pronounced skew can be observed, especially in the imaginary parts, while the real part spread is dominant.

V. Global Variability of the Power Amplifier

Combining the X-par model and the MDIF model for the active and passive structures, respectively, the full Monte

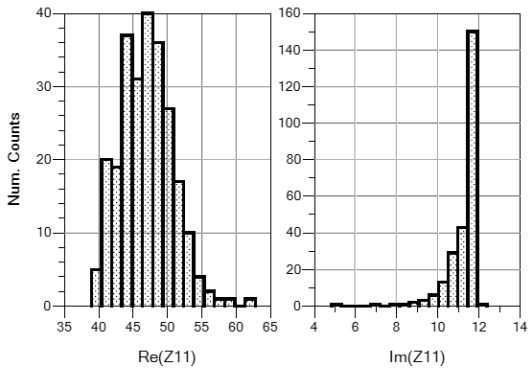

Fig. 9. Real and imaginary parts of the load impedance resulting from a random MIM layer thickness with a Gaussian distribution of 2% standard deviation.

Carlo analysis of the global stage is readily available within ADS. The simulation time is extremely low, since all models are essentially based on lookup tables, parametrized on the technological parameters subject to statistical variations. Hence, the numerical burden is similar to a stand-alone *circuit* Monte Carlo analysis, with the only overhead of parameter interpolation.

Fig. 10 shows the results of a Monte Carlo analysis with a random Gaussian distribution separately of the device doping (black histograms), and of the MIM dielectric layer thickness, at various input powers. In both cases the standard deviation of the statistical distribution is 2% of the nominal value, well within the technological expectations. In particular, the doping variations in a MMIC implementation can be regarded as more limited if several stages are close one to the other on the same wafer (also in the perspective of a combined stage), while they can be more severe across the wafer or if a wafer-to-wafer variability is considered. Noticeably, the overall spread is dominated by doping variations, even if at intermediate input power, where we already noticed the larger variability, the two contributions are almost comparable. At larger input power, the spread is compressed. At lower input power the overall spread exhibits the previously noticed skew. Since the impedance synthesized with the matching network already exhibits a skew as a function of the MIM layer thickness, the MIM related spread is even more significantly skewed at all power levels, while the doping related one follows the previously analyzed pattern.

Finally, the overall spread of concurrent uncorrelated variations of doping and dielectric layer thickness is considered. Fig. 11 shows that the overall spread is significantly increased, especially at intermediate power (the only value shown in the graph): the table in the figure reports the output power standard deviations due to the separate contributions, together with the overall value. Nearly 30% of the overall variance is due to the passive elements at this intermediate input power level.

VI. Conclusion

We presented an efficient CAD approach to perform the sensitivity and statistical variability analysis of RF/microwave

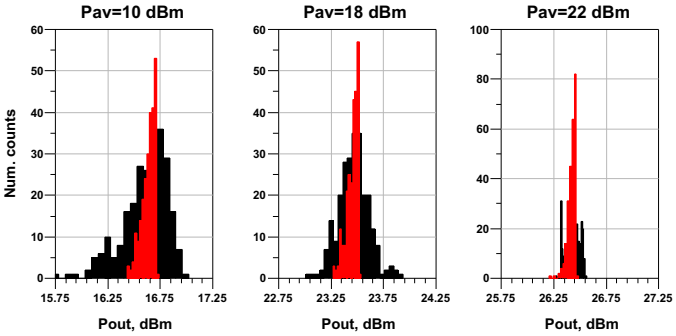

Fig. 10. Output power distribution of the PA stage subject to doping variations (black) and MIM layer variations (red) at different input power levels.

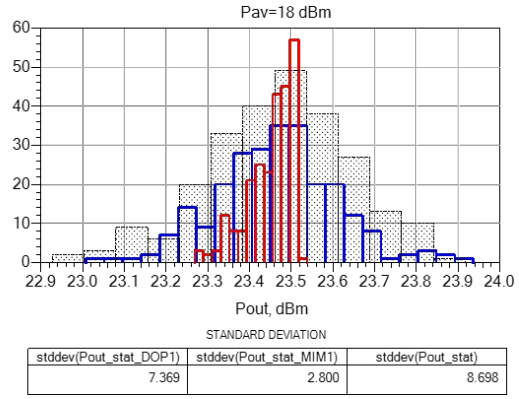

Fig. 11. Output power distribution of the PA stage subject to concurrent doping variations (black) and compared to the separate doping (blue) and MIM layer variations (red).

nonlinear stages with respect to variations of the technological and/or physical parameters of the active and passive components of the stage. The approach is based on lookup table models (X-pars and parametrized S-parameters for the active and the passive part, respectively) gathered through a limited number of off-line PB and EM simulations, which retain direct link with the process parameters. These models are then effectively interpolated in circuit-level simulations allowing for a fast, physically-reliable statistical analysis. The accuracy of the proposed approach is demonstrated through direct Monte Carlo simulations of a deep class AB amplifier in III-V MESFET technology, where variability vs. the active device doping and passive MIM dielectric thickness is considered, showing that the proposed interpolation approach is highly accurate. The concurrent circuit-level variability simulation is carried out within the ADS EDA tool with a negligible computational burden.

The overall variability is shown to strongly depend on input power, with larger spread at intermediate values. Despite the fundamental technology variations are always assumed symmetrically distributed around the average value, a pronounced skew towards lower output power is present, partly due to the stage nonlinearity and partly because of the behavior of the loads synthesized by the external passive part. The active device variability generally dominates the one of the passive structure, despite the contribution to the overall variance due to the passives turns out to be important at specific input power drives. These results are emblematic of the complex interplay among variations in nonlinear stages, requiring multiphysics simulations.

ACKNOWLEDGMENT

This work has been supported by the Italian Ministero dell'Istruzione dell'Università e della Ricerca (MIUR) under the PRIN 2017 Project "Empowering GaN-on-SiC and GaN-on-Si technologies for the next challenging millimeter-wave applications (GANAPP)"

REFERENCES

[1] S. Khandelwal, *Physics-based Compact Models: An Emerging Trend in Simulation-based GaN HEMT Power Amplifier Design* , 2019 IEEE 20th Wireless and Microwave Technology Conference (WAMICON), 8-9 April 2019 Cocoa Beach (FL), USA.

[2] I. Angelov, H. Zirath, N. Rorsmann, *A New Empirical Nonlinear Model for HEMT and MESFET Devices*, IEEE Transactions on Microwave Theory and Techniques, vol. 40, no. 12, pp. 2258–2266, Dec. 1992.

[3] F. Jazaeri and J.-M. Sallese, *Charge-Based EPFL HEMT Model*, IEEE Trans. El. Dev., Vol. ED-66, No. 3, pp. 1218–1229, March 2019.

[4] Z. Wen, S. Mao, Y. Wu, R. Xu, B. Yan ; Y. Xu, *A Quasi-Physical Large-Signal Statistical Model for 0.15 μm AlGaN/GaN HEMTs Process*, 2019 IEEE MTT-S International Microwave Symposium Digest, pp. 204-207, 2–7 June 2019, Boston (MA), USA.

[5] J. C. Pedro, D. E. Root, J. Xu, L. Cótimos Nunes, *Nonlinear Circuit Simulation and Modeling: Fundamentals for Microwave Design*. Cambridge University Press, 2018.

[6] D. E. Root, J. Verspecht, J. Horn, M. Marcu, *X-parameters*. Cambridge University Press, 2013.

[7] https://www.keysight.com/main/application.jspx?nid=-34017.0.00

[8] F. Bonani, S. Donati Guerrieri, G. Ghione, M. Pirola, *A TCAD approach to the physics-based modeling of frequency conversion and noise in semiconductor devices under large-signal forced operation*, IEEE Trans. Electron Devices, vol. 48, no. 5, p. 966, 2001.

[9] F. Bertazzi, F. Bonani, S. Donati Guerrieri, G. Ghione, *Physics-based SS and SSLS variability assessment of microwave devices through efficient sensitivity analysis*, 2012 Workshop on Integrated Nonlinear Microwave and Millimetre-Wave Circuits (INMMIC), Dublin, Ireland, 3–4 September 2012.

[10] F. Bonani; S. Donati Guerrieri, G. Ghione, *Compact conversion and cyclostationary noise modeling of pn-junction diodes in low-injection. Part I. Model derivation*, IEEE Trans. El. Dev., Vol. ED-51, No: 3, pp. 467–476, March 2004.

[11] F. Bonani; S. Donati Guerrieri, G. Ghione, *Compact conversion and cyclostationary noise modeling of pn-junction diodes in low-injection. Part II. Discussion*, IEEE Trans. El. Dev.,Vol. ED-51, No: 3, pp. 477–485, March 2004.

[12] M. Rudolph; F. Bonani, *Low-frequency noise in nonlinear systems*, IEEE Microwave Magazine, Vol. 10, No. 1, pp. 84–92, February 2009.

[13] S. Donati Guerrieri, F. Bonani; F. Bertazzi; G. Ghione, *A Unified Approach to the Sensitivity and Variability Physics-Based Modeling of Semiconductor Devices Operated in Dynamic Conditions. Part I: Large-signal sensitivity*, IEEE Trans. El. Dev., Vol. ED-63, No. 3, pp. 1195–1201, March 2016.

[14] S. Donati Guerrieri, F. Bonani; F. Bertazzi; G. Ghione, *A Unified Approach to the Sensitivity and Variability Physics-Based Modeling of Semiconductor Devices Operated in Dynamic Conditions. Part II—Small-Signal and Conversion Matrix Sensitivity*, IEEE Trans. El. Dev., Vol. ED-63, No: 3, pp. 1202–1208, March 2016.

[15] S. Donati Guerrieri, F. Bonani; M. Pirola, *Concurrent Efficient Evaluation of Small-Change Parameters and Green's Functions for TCAD Device Noise and Variability Analysis*, IEEE Trans. El. Dev., Vol. ED-64, No: 3, pp.1269–1275, Feb. 2017.

[16] S. Donati Guerrieri, F. Bonani and G. Ghione, *Linking X Parameters to Physical Simulations for Design-Oriented Large-Signal Device Variability Modeling*, 2019 IEEE MTT-S International Microwave Symposium Digest, 2–7 June 2019, Boston (MA), USA.

[17] D. Lamey, L. Zhang, H. Rueda, H. Kabir, R. Sweeney and K. Kim, *Device physics and EM simulation based modeling methodology for LDMOS RF power transistors*, 2017 IEEE MTT-S International Conference on Numerical Electromagnetic and Multiphysics Modeling and Optimization for RF, Microwave, and Terahertz Applications (NEMO), Seville, 2017, pp. 79–81.
[18] F. Bertazzi, F. Cappelluti, S. Donati Guerrieri, F. Bonani and g, Ghione, *Self-Consistent Coupled Carrier Transport Full-Wave EM Analysis of Semiconductor Traveling-Wave Devices* , IEEE Transactions on Microwave Theory and Techniques, Vol. 54, No. 4, pp. 1611–1618, April 2006
[19] *https://www.keysight.com/main/editorial.jspx?cc=US&lc=eng&ckey=1619575&nid=-34346.1255256.08&pid=2952481*
[20] *https://www.awr.com/software/products/ni-awr-design-environment*
[21] J. Verspecht, D.F. Williams, D. Schreurs, K.A. Remle, M.D. McKinley, *Linearization of large-signal scattering functions*, IEEE Trans. Microw. Theory Tech., vol. 53, no. 4, p. 1369–1376, 2005.
[22] S. A. Maas, *Microwave mixers*. Artech House, 1992.
[23] S. Donati Guerrieri, F. Bonani, and G. Ghione, *A novel approach to microwave circuit large-signal variability analysis through efficient device sensitivity-based physical modeling*, Int. Microwave Symp. (IMS 2016), 22-27 May 2016, San Francisco, CA, USA.

PLACE PHOTO HERE

Simona Donati Guerrieri SIMONA DONATI GUERRIERI received the Laurea degree in physics in 1993 and the Ph.D. degree in electron devices in 1999. Since 2001 she has been with the Politecnico di Torino, Turin, Italy, where she is currently an Associate Professor of Electronics. Her current research interests include modeling of solid-state devices, including nonlinear noise and variability, and microwave integrated circuit design.

PLACE PHOTO HERE

Chiara Ramella CHIARA RAMELLA received the M.S degree in electronic engineering and the Ph.D. degree in electronic devices from the Politecnico di Torino, in 2009 and 2013, respectively. She is currently an Assistant Professor with the Politecnico di Torino. Her current research interests include RF/microwave MMIC design and measurments.

PLACE PHOTO HERE

Fabrizio Bonani FABRIZIO BONANI received the Laurea (cum laude) and Ph.D. degrees in electronics engineering from the Politecnico di Torino, Turin, Italy, in 1992 and 1996, respectively. He is currently a Full Professor of Electronics with the Politecnico di Torino. His current research interests include modeling and design of semiconductor devices, stability and noise analysis of nonlinear circuits, and development of innovative devices for unconventional computation.

PLACE PHOTO HERE

Giovanni Ghione GIOVANNI GHIONE is Full Professor in Electronics since 1990, now with Politecnico di Torino. His research activity concerns the fields of microwave electronics, physics-based compound semiconductor (III-V and widegap) device simulation, modeling of optoelectronic devices (modulators, FIR and NIR detectors, solar cells). He has authored or co-authored more than 300 research papers on the above subjects and five books.